

THE STRUCTURE OF POROUS AND SPONTANEOUSLY DENSIFIED AMORPHOUS PbSiO₃: A MOLECULAR DYNAMICS STUDY

KATARZYNA CHOMENKO¹, GRZEGORZ BERGMAŃSKI¹, MICHAŁ BIAŁOSKÓRSKI^{1,2}
 MONIKA RYCHCIK-LEYK¹, SANDRO FELIZIANI³, SANDRO FRIGIO³
 AGNIESZKA WITKOWSKA^{1,2}, AND JAROSŁAW RYBICKI^{1,2}

¹ Department of Solid State Physics, Faculty of Technical Physics and Applied Mathematics
Gdansk University of Technology, Narutowicza 11/12, 80-952 Gdansk, Poland

² TASK Computer Centre, Narutowicza 11/12, 80-952 Gdansk, Poland

³ Istituto di Matematica e Informatica, Università di Camerino
Camerino (MC), Italy

(Rec. 6 May 2004)

Abstract: In the paper we propose and test a "gel-drying" method of obtaining porous oxide glasses in Molecular Dynamics (MD) simulations. The simulation is started with low (screened) values of ionic charges. Then, the charges are gradually increased (to mimic the gradual elimination of a polar solvent) up to full ionic charges (a completely dry gel). This computational trick is applied to produce a porous PbSiO₃ system. The structure of the resulting low-density samples is analysed in detail. Then, the porous structures are submitted to spontaneous densification, and the structure of the obtained dense bulk glasses is analysed. Finally, the structures of bulk glass obtained *via* spontaneous densification (density $\rho = 8250 \text{ kg/m}^3$) and bulk glass of the same density obtained *via* isotropic compression are compared.

1. INTRODUCTION

The classical Molecular Dynamics (MD) method [1-5] consists in a numerical solution of equations of motion of many interacting particles. In the case of bulk amorphous solids a cubic simulation box is usually used, with periodic boundary conditions along the *xyz* directions. The initial particle positions are often generated using the skew start method [5], whereas the initial velocities are generated at random from the Maxwell distribution of the desired temperature. The direct simulation results are the positions and velocities of all the particles at each time-step. The obtained atomic configurations can be subjected to a structural analysis, while proper averaging along the trajectories yields the thermodynamic parameters of the simulated system.

In order to simulate the structure of oxide glasses, Born-Mayer-Huggins potentials with full ionic charges are often used. Usually, the glass is initially prepared as hot melt (at the temperature of the order of 10^4 K) which is then slowly cooled (e.g. at the rate of 10^{13} K/s) to room temperature. However, the above-mentioned procedure does not work if one wants to simulate low density (porous) phases of ionic systems, in which case a special approach must

be developed. The problem is that while having to interatomic potentials like the Born-Mayer-Huggins ones at our disposal, with full ionic charges, correctly reproducing the bulk properties of a given material at normal density, and starting a constant-volume simulation at low density (e.g. 10-20 times lower than the normal density), the periodicity readily breaks and one obtains a single, roughly spherical cluster of normal (or somewhat higher) density. In order to obtain a porous medium one can mimic a kind of fictive "gel drying", i.e. to start the simulation with low ionic charges (screened by a fictitious polar solvent) and slowly increase them to reach their full nominal ionicity. The fictive solvent molecules are not simulated: their presence appears only in the charge screening of the gel ions. In such a way one can obtain a "porous material".

The obtained porous samples, when further simulated under isobaric conditions with null external pressure, densify spontaneously (collapse). During such densification a great amount of thermal energy is released at the cost of a decrease in potential energy. Therefore, the system must be cooled in the process, e.g. by direct velocity scaling.

In this paper we test our "gel-drying" method for the PbSiO_3 system. This choice is justified by the fact that we have already published a series of papers on the structure of lead-silicate glasses [6-9], so that the present structural results on low density and collapsed phases can be compared with the structure of normal-density and slightly compressed or expanded samples of the same chemical composition.

The paper is organised as follows. In Section 2 we describe in general the simulations we have performed and present the raw simulation results. In Section 3 the short- and medium-range structures of the obtained low density phases are described. Spontaneous gel densification and the structure of the resulting dense glass are described and compared with the structure of the low density phase in Section 4. In the same Section the present results obtained with the "gel drying" technique and spontaneous densification are confronted with the structure of glasses obtained previously with the melt cooling technique. Section 5 contains our concluding remarks.

2. GENERAL CHARACTERISTICS OF THE PERFORMED SIMULATIONS AND METHODS OF STRUCTURAL ANALYSIS

The simulation box contained 2500 particles: 500 Pb^{+2} ions, 500 Si^{+4} ions and 1500 O^{-2} ions. The box edge length, B_l , was density dependent: for the density of 300 kg/m^3 $B_l = 46.1036 \text{ \AA}$, for the density of 600 kg/m^3 $B_l = 36.5925 \text{ \AA}$, for the density of 1200 kg/m^3 $B_l = 29.0435 \text{ \AA}$ and for the density of 3000 kg/m^3 $B_l = 21.3994 \text{ \AA}$. Since the density of the PbSiO_3 glass at normal conditions is 5970 kg/m^3 , the considered structures are about 20, 10, 5 and 2 times less dense. Periodic boundary conditions were applied along the xyz directions. The particles were assumed to interact according to the Born-Mayer-Huggins potential:

$$\phi(r) = A_{ij} \exp[B_{ij}(\sigma_{ij} - r)] - \frac{C_{ij}}{r^6} + \frac{Q_i Q_j}{4\pi\epsilon_0 r}, \quad (1)$$

where i and j are the indices of the atomic species (Pb, Si, O). The coefficient values are reported in Table 1.

Table 1. Coefficient values of potential (1) [10]

Coefficient	Pb-Pb	Pb-Si	Pb-O	Si-Si	Si-O	O-O
$A_{ij} [\times 10^{20}] \text{ J}$	0.1014	8.45	5.915	6.76	4.225	1.69
$B_{ij} [\text{\AA}^{-1}]$	3.448	3.448	3.448	3.448	3.448	3.448
$C_{ij} [\text{J} \cdot \text{\AA}^6]$	0.0	0.0	0.0	0.0	0.0	0.0
$\sigma_{ij} [\text{\AA}]$	2.440	2.368	2.640	2.296	2.568	2.840

The most important feature of the present simulations was a gradual increase of the ionic charges, from 10% of the full ionic charge up to the full ionic charge, with a 10% step (ten subsequent charge states). The same computational scheme was applied each charge state: thermalisation to room temperature (300 K) using temperature scaling over 30000 time steps, and the system sampling over 10000 time steps. Thus, the final particle configurations of low density (porous) systems (see Fig. 1) were obtained after 400000 steps (time step, $\Delta t = 10^{-15} \text{ s}$). Then, the final low density atomic configurations were used as initial configurations for further simulations under the (NpT) conditions with null external pressure. The initial porous systems collapsed spontaneously, and uniform bulk glasses of high density were obtained.

In our simulations an extremely "delicate" temperature scaling scheme was applied: the velocities were scaled to nominal temperature $T_{\text{nom}} = 300 \text{ K}$ only if the rolling average of temperature, calculated from the moment of the previous scaling, went beyond the $(T_{\text{nom}} - \Delta T, T_{\text{nom}} + \Delta T)$ with $\Delta T = 100 \text{ K}$ interval. Usually, the last temperature scaling occurred before step 20000 of the thermalisation runs. In consequence, the temperature during the sampling runs was somewhat different (by several K) from T_{nom} . The simulations were performed using the mdsim code [11]. The only structural information directly accessible after execution of the simulation program are the pair radial distribution functions (RDFs).

To describe quantitatively the obtained RDFs, Γ -like profiles have been used [12-14]:

$$f(r) = \frac{2N}{\sigma|\beta|\Gamma(4\beta^{-2})} \left[4\beta^{-2} + \frac{2(r-R)}{\beta\sigma} \right]^{(4\beta^{-2}-1)} \exp\left[-\left(4\beta^{-2} + \frac{2(r-R)}{\beta\sigma} \right)\right], \quad (2)$$

where N is the coordination number, R - average distance, σ - standard deviation, β - the skewness parameter.

A more detailed analysis of the final atomic configurations has been performed using a number of tool programmes, contained in the anelli package [15-17]. In order to characterize

quantitatively the disorder degree of tetrahedral SiO₄ structural units we have used the following shape estimators:

$$\stackrel{\tau}{T} \underline{L}^V = \frac{-A - 0}{tfI} A \cdot A \cdot i^j , \quad (3)$$

$$7 = \hat{\wedge}_{L=1}^{\infty} \frac{(-a - A)^{-\frac{1}{2}}}{\frac{1}{2} \hat{\wedge}_{A=A}^{00} A \cdot A} + \hat{\wedge}_{L=1}^{\infty} \frac{(-C - A)^{-\frac{1}{2}}}{\frac{1}{2} \hat{\wedge}_{C=C}^{00} C \cdot A}, \quad (4)$$

where C and A stand for cations and anions, respectively, O_{C-C} and O_{C-A} mean the average C-C and C-A distances, respectively, and $/c-c,L$, $/c-a,l$ denote the actual C-C and C-A distances for the L-th edge of a polyhedron. For ideal polyhedra the values of T_2 and T_3 parameters equal zero, whereas for distorted structures they assume positive values.

Kolorowa rycina

Fig. 1. Atomic configurations at the last time step of the simulations for $p = 300 \text{ kg/m}^3$ (upper left), $p = 600 \text{ kg/m}^3$ (upper right), $p = 1200 \text{ kg/m}^3$ (lower left), $p = 3000 \text{ kg/m}^3$ (lower right). Blue balls - Pb atoms, red balls - O atoms, green balls - Si atoms

The distribution of the T values can be calculated for the final MD-simulated structures. In order to interpret such distributions we compare them with reference data, obtained in the following way. Assuming the cation position to be fixed, we shift at random tetrahedron vertices within small cubes (centred on the ideal anion positions) of edge-lengths equal to a certain fraction q of tetrahedron's edge, L . For tetrahedra distorted in this way, one can calculate the corresponding T values. By repeating the distortion-and- T -calculation cycle many times (e.g. 10^6 times) for many values of q , one gets a q -dependent family of T distributions. The reference data thus obtained for shape estimators (3) and (4) are shown in Fig. 2. Now, using the minimum square difference criterion, one can individuate a q value that produces the T distribution best conforming to the MD-simulated T distribution. This means that the distortion degree of tetrahedra (in our case the SiO_4 structural units) can be characterized quantitatively with a single parameter - the best fit value of q .

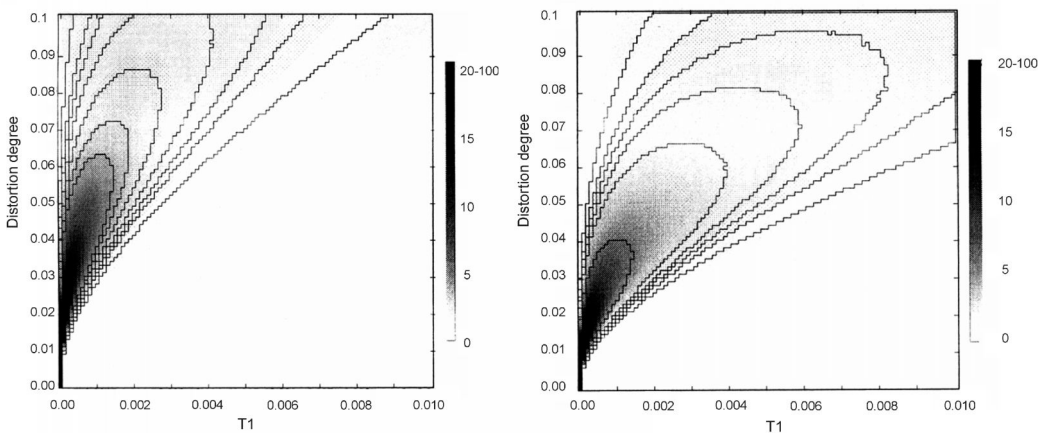


Fig. 2. T_1 and T_2 value distributions in the function of the q parameter

Partial RDFs (i.e. Si-Si, Si-Pb and Pb-Pb spatial correlations) could be used to describe the medium-range structure (mutual arrangement of CA_n structural units, C - cation, A - anion). However, interpretation of these correlations is ambiguous, and the cation-anion ring statistics seem to better characterize the medium-range structure better. The basal cation-anion rings have been calculated using the Balducci-Perlman-Mancini algorithm [15-20].

3. THE STRUCTURE OF LOW DENSITY SYSTEMS

The first two subsections are dedicated to the structure of Si^{+4} and Pb^{+2} cation environments, respectively. The medium-range order is characterised in the third subsection.

3.1. Si^{+4} ion environment

Figures 3 and 4 show the first peaks of partial radial distribution functions, $g_{\text{Si-O}}(r)$ and $g_{\text{O-O}}(r)$ for structures of various densities. Also shown are the peaks' components, approxi-

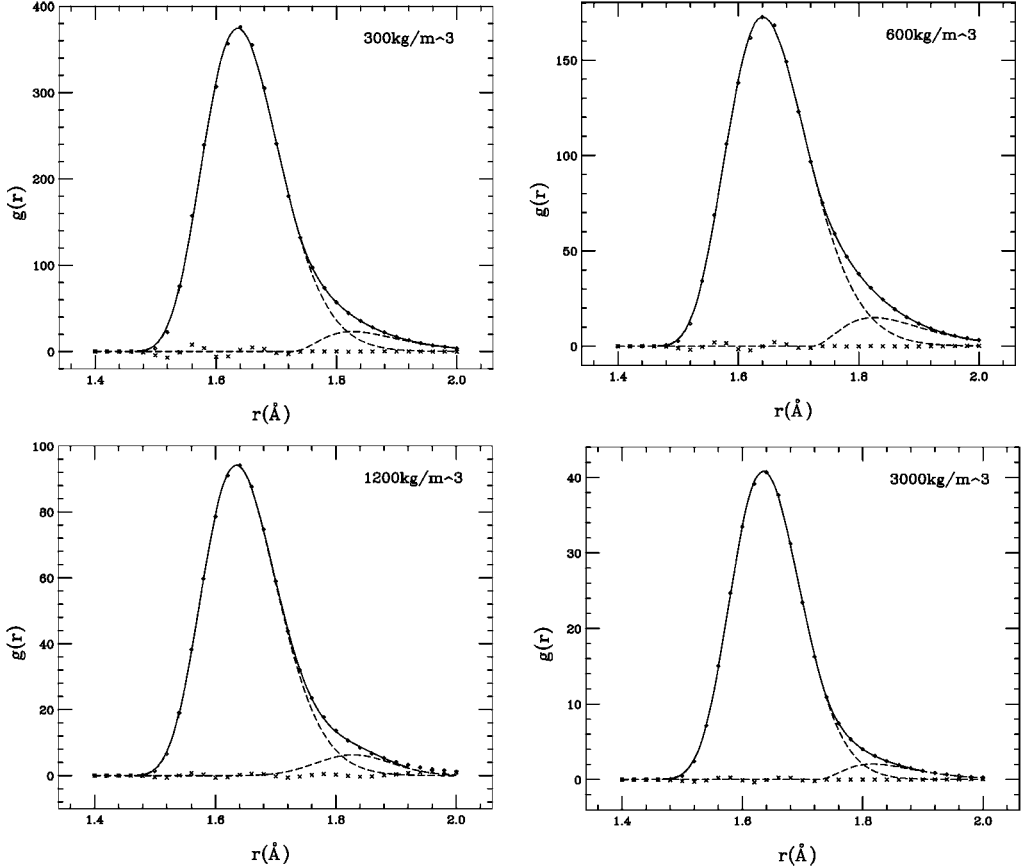


Fig. 3. Si-O radial distribution functions in systems of various densities

Table 2. Structural parameters of the first maximum of the Si-O spatial correlation

ρ [kg/m ³]	R [\AA]	N	σ^2 [\AA ²]	β	N_c
300	1.66	3.935	0.004	0.507	4.257
	1.87	0.321	0.006	1.065	
600	1.66	3.878	0.005	0.535	4.325
	1.88	0.447	0.007	1.089	
1200	1.66	3.847	0.004	0.488	4.165
	1.84	0.317	0.004	0.103	
3000	1.65	3.882	0.004	0.388	4.145
	1.86	0.263	0.005	1.093	

mated with Γ -like functions (2), together with the fitting residua. The corresponding values of the R , σ , β and N structural parameters are compiled in Tables 2 and 3.

The Si-O correlations show a sharp first peak for all the densities, with the most probable distance of 1.64 Å, the same as in the normal-density glass [6, 7, 10]. A more detailed analysis of the first peaks has revealed the existence of two fractions of bond-lengths (see Fig. 3 and Table 2).

Let us now discuss the first, main peak. The average Si-O distances amount to about 1.66 Å for all the densities. The corresponding coordination numbers are equal to 4, with an accuracy of 4%. The most probable O-Si-O angles equal to 104-107° (see Fig. 5), and are thus close to 109°, characteristic of an ideal SiO₄ tetrahedron. Assuming the SiO₄ unit to be tetrahedral, with the Si-O distance of 1.65 Å, the O-O distance should equal 2.65 Å (cf. Fig. 3 and Table 2), and of course the O-O-O angle should equal 60° (cf. Fig. 5). The σ^2 parameter of the main Si-O subpeak of the first peak is almost independent of density. Thus, the vibrational amplitude of the Si-O bond, taken together with the structural disorder, only weakly depends on the system's density.

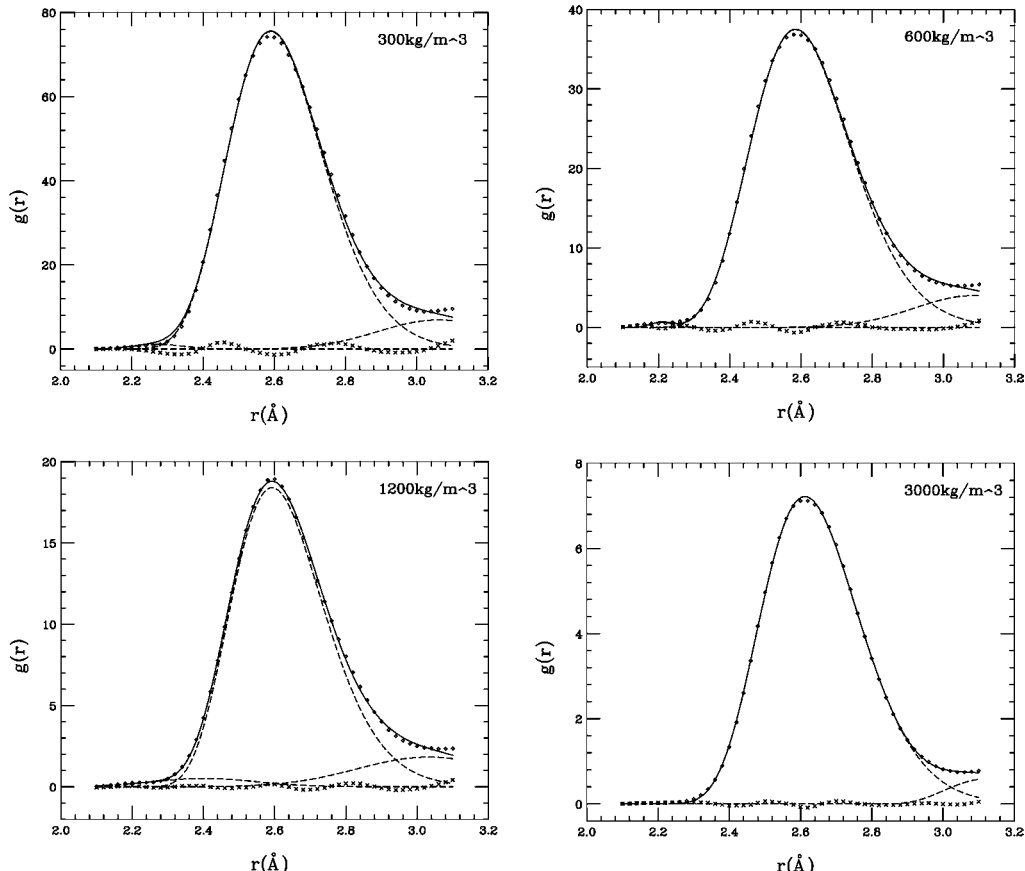


Fig. 4. O-O radial distribution functions in systems of various densities

Table 3. Structural parameters of the first maximum of the O-O spatial correlation

ρ [kg/m ³]	R [\AA]	N	σ^2 [\AA ²]	β	N_c
300	2.28	0.025	0.005	0.104	4.944
	2.64	4.238	0.02	0.473	
	3.09	0.681	0.03	0.1	
600	2.21	0.012	0.001	0.108	5.167
	2.64	4.4	0.022	0.511	
	3.1	0.755	0.027	0.001	
1200	2.43	0.106	0.022	0.102	4.93
	2.64	4.005	0.019	0.563	
	3.06	0.819	0.04	0.032	
3000	2.66	4.267	0.022	0.519	4.771
	3.2	0.504	0.022	0.709	

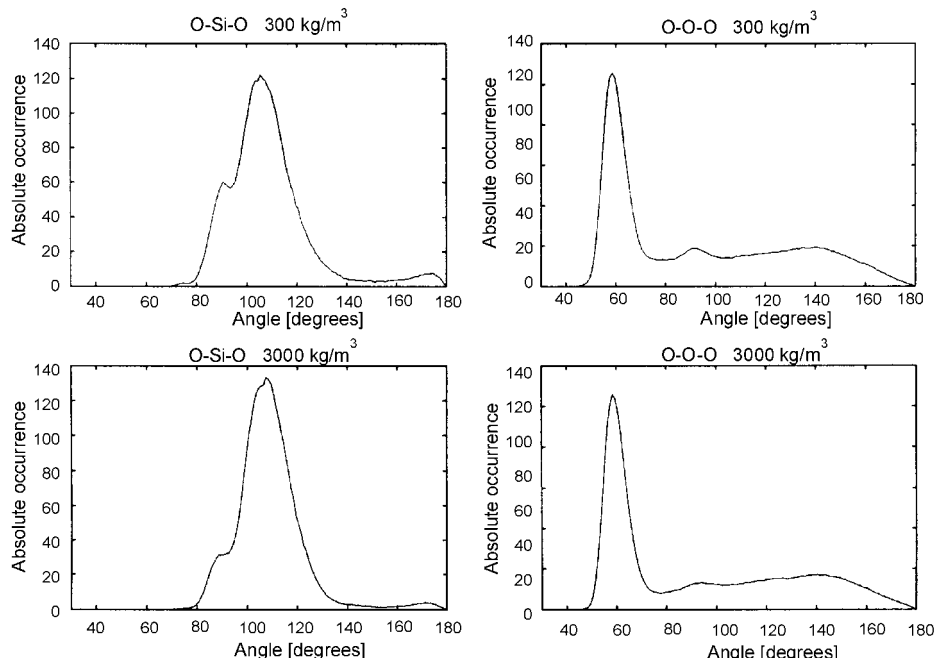


Fig. 5. Angular O-Si-O and O-O-O distribution functions for systems of various densities

As far as the second subpeak is concerned, the related average Si-O distance amounts to 1.86 Å for all the densities, whereas the corresponding coordination numbers range from 0.32 to 0.45, so that the total Si-O coordination number for the first RDF maximum exceeds 4. This

means that a small fraction of Si ions have the fifth oxygen neighbour at the distances centred about 1.86 Å.

Now, an explanation of the existence of the O-Si-O angle equal of 90° (see Fig. 5) can be given. This angle appears in the triangles formed by perpendicular Si-O bonds 1.86 Å long (the second Si-O subpeak), where the O-O distance amounts to 2.66 Å (the average O-O distance). The occurrence probability of such triangles decreases with increasing density, and the changes are related to the decreasing occurrence probability of five-fold coordination of Si ions by oxygen ions. Simultaneously, the decreasing (with increasing density) contribution of the 90° O-O-O angles might suggest that, with increasing density, the SiO₅ units change from pyramids with a square base to triangular bipyramids (Fig. 5).

The average O-O distances in the second subpeak amount to about 3.1 Å, and the corresponding coordination numbers range from 0.5 to 0.8. The O-O distances centred around 3.1 Å are related with PbO_n structural units and do not appear within the nearest neighbourhood of the silicon ions. However, a tiny pre-peak in the O-O spatial correlation does appear. Here, the average O-O distances range from 2.21 Å to 2.43 Å. The related coordination number is very low (from 0.01 to 0.1). Since the left wing of the main O-O peak significantly overlaps with the considered pre-peak, its complete and unequivocal interpretation is impossible. However, we have identified those O-O pairs that contribute to the left wing of the pre-peak as belonging to the SiO₅ units.

The distribution of coordination numbers for the Si-O pair, calculated with a cut-off radius of 2 Å, is as follows: with increasing density, from 74% to 88% of Si ions have four oxygen neighbours and from 25% to 12% - five oxygen neighbours. The fraction of three-fold and six-fold coordinations does not exceed 1%. All the SiO₄ groups show the tetrahedral symmetry. Distributions of the values of the T_1 and T_2 parameters have been calculated, and in both cases the best fit value of q equals 0.05. This means that in the simulated SiO₄ tetrahedra vertex dispersion around the ideal positions is of order of 2.5% of the average O-O distance. Such a high deformation degree is mainly due to the structural disorder in the free surface built from the faces of the SiO₄ tetrahedra (see Fig. 1).

3.2. Pb⁺² ions environment

The most probable Pb-O distance amounts to 2.3 Å for all the considered densities. The Pb-O radial distribution functions are shown in Fig. 6, whereas their structural parameters are listed in Table 4.

The two fractions of bond lengths cannot be related to any single dominating structural unit. A detailed analysis of the distribution of Pb-O coordination numbers (conducted with a cut-off radius of 3.0 Å) has revealed a wide spectrum of Pb local neighbourhoods. The fraction of PbO₄ units increases slightly with increasing density, from 33% to 42%. The PbO₄ units fall into two classes: tetrahedron-like (Pb belongs to a tetrahedron spanned by four oxygen neighbours) and pyramid-like (Pb does not belong to the tetrahedron spanned by four

oxygen neighbours). The fraction of the tetrahedron-like structures increases with increasing density from 32% for $\rho = 300 \text{ kg/m}^3$ to 62% for $\rho = 3000 \text{ kg/m}^3$.

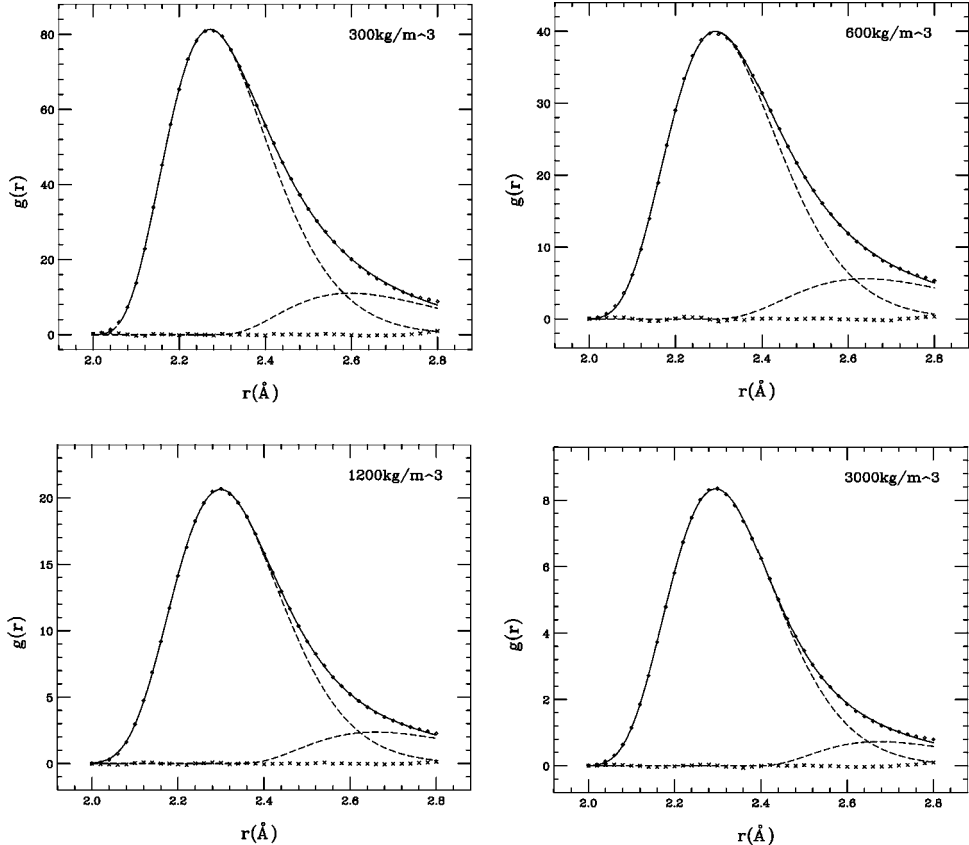


Fig. 6. Pb-O radial distribution functions in systems of various density

Tab. 4. Structural parameters for the Pb-O pair

ρ [kg/m ³]	R [\AA]	N	σ^2 [\AA ²]	β	N_c
300	2.34	3.23	0.018	0.751	4.133
	2.74	0.903	0.05	0.995	
600	2.36	3.44	0.02	0.691	4.491
	2.79	1.049	0.06	0.956	
1200	2.35	3.46	0.018	0.604	4.299
	2.8	0.84	0.053	0.98	
3000	2.36	3.5	0.019	0.655	4.084
	2.8	0.58	0.043	1.022	

PbO_3 units' contribution is quite significant: from 20% for $\rho = 300 \text{ kg/m}^3$ to 28% for $\rho = 3000 \text{ kg/m}^3$). The PbO_3 groups have been identified as distorted triangles. The average distance between a Pb ion and the plane determined by the three neighbouring oxygen ions decreases with increasing density (from 0.6 Å for 300 kg/m^3 to 0.4 Å for 3000 kg/m^3). Thus, at higher densities the PbO_3 triangles are somewhat flatter. PbO_5 units, identified as triangular bipyramids, contribute from about 30% for $\rho = 300 \text{ kg/m}^3$ to about 20% for 3000 kg/m^3 . The fraction of square bipyramids, PbO_6 does not exceed 10%. 2-, 7-, and 8-fold oxygen coordinations of Pb occur rarely; their total contribution is less than 3%.

3.3. Medium-range order

In order to get some insight into the mutual orientation of CA_n units, one can consider the cation-cation spatial correlations. The first RDF maxima for the Si-Si, Pb-Pb and Pb-Si pairs have very complex structures and no clear and univocal information on the medium-range order can be extracted. However, ring analysis allows us to get some insight into the mutual arrangement of the SiO_n and PbO_n structural units.

The Si-O-Si-O-... rings' statistics are shown in the upper part of Fig. 7. Four-member rings dominate for all the densities, but three- and five-member rings are also frequent. For $\rho \geq 600 \text{ kg/m}^3$ some (no more than 5%) 2-member rings appear - they correspond to edge-sharing SiO_4 tetrahedra. In general, the obtained ring length distribution is obviously shifted towards the shorter rings in respect of pure silica, where 6-, 7- and 8-member rings dominate. This is due to the presence of Pb ions in the structure.

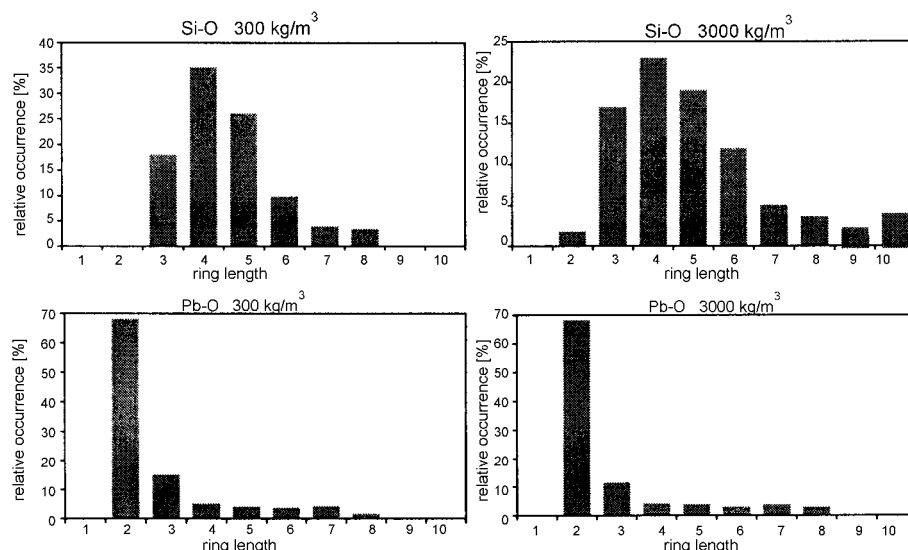


Fig. 7. Length distributions of Si-O-Si-O-... and Pb-O-Pb-O-... rings in systems of various densities

The statistics of Pb-O-Pb-O... rings are shown in the lower part of Fig. 7. 2-member rings dominate (63-68%) for all the densities. This means that most PbO_n units usually share their edges, in contradistinction to the SiO_4 tetrahedral units, for which edge-sharing is very rare.

4. SPONTANEOUS COLLAPSE OF LOW DENSITY STRUCTURES AND THE STRUCTURE OF THE RESULTING BULK GLASS

Spontaneous densification of the low density systems has been realized as an (NpT) run, with null external pressure, restarted from the atomic configuration at the last time step of the (NVT) simulation at low density. The time-dependence of density during the process is shown in Fig. 8. The final bulk glasses have a very high density of 8000-9000 kg/m³. Their structures are very similar, therefore we shall concentrate on only one of the high-density systems ($\rho = 8250 \text{ kg/m}^3$), obtained from a system of initial density equal to 1200 kg/m³.

Spatial correlations between all the atomic pairs are shown in the left-hand columns of Figs. 9 and 11 and the related structural parameters are listed in Table 5.

The Si-O radial distribution functions in the collapsed porous systems have sharp peaks with average Si-O distances of 1.71 Å, i.e. about 0.05 Å longer than in low-density and normal-density PbSiO_3 glasses. The distribution of Si-O coordination numbers is as follows: 33%, 57% and 10% of all Si atoms have 4-fold, 5-fold and 6-fold oxygen coordination, respectively. Other coordinations are absent. 98% of SiO_4 groups have a tetrahedron-like form. The best-fit value of q is about 0.08, higher than in the low density systems. The length distribution of Si-O-Si-O... rings is significantly different from that shown in Fig. 7 for low densities: the contributions of 3- and 4-member rings exceed 20%, the contribution of 2-member rings increased to more than 10%, while the contribution of 5-member rings is decreased to about 10%. The frequencies of the longer rings in the collapsed glass are similar to those in the low density systems.

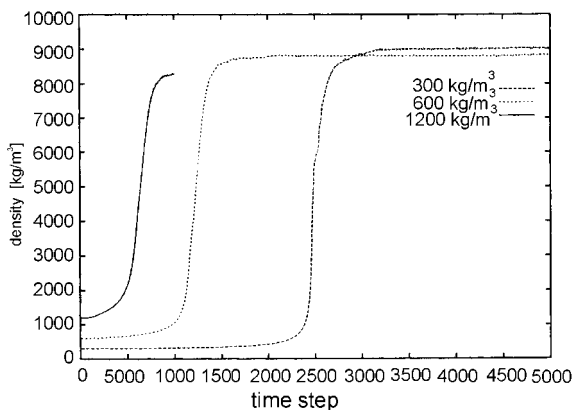


Fig. 8. Time dependence of the system density during spontaneous densification for various initial densities

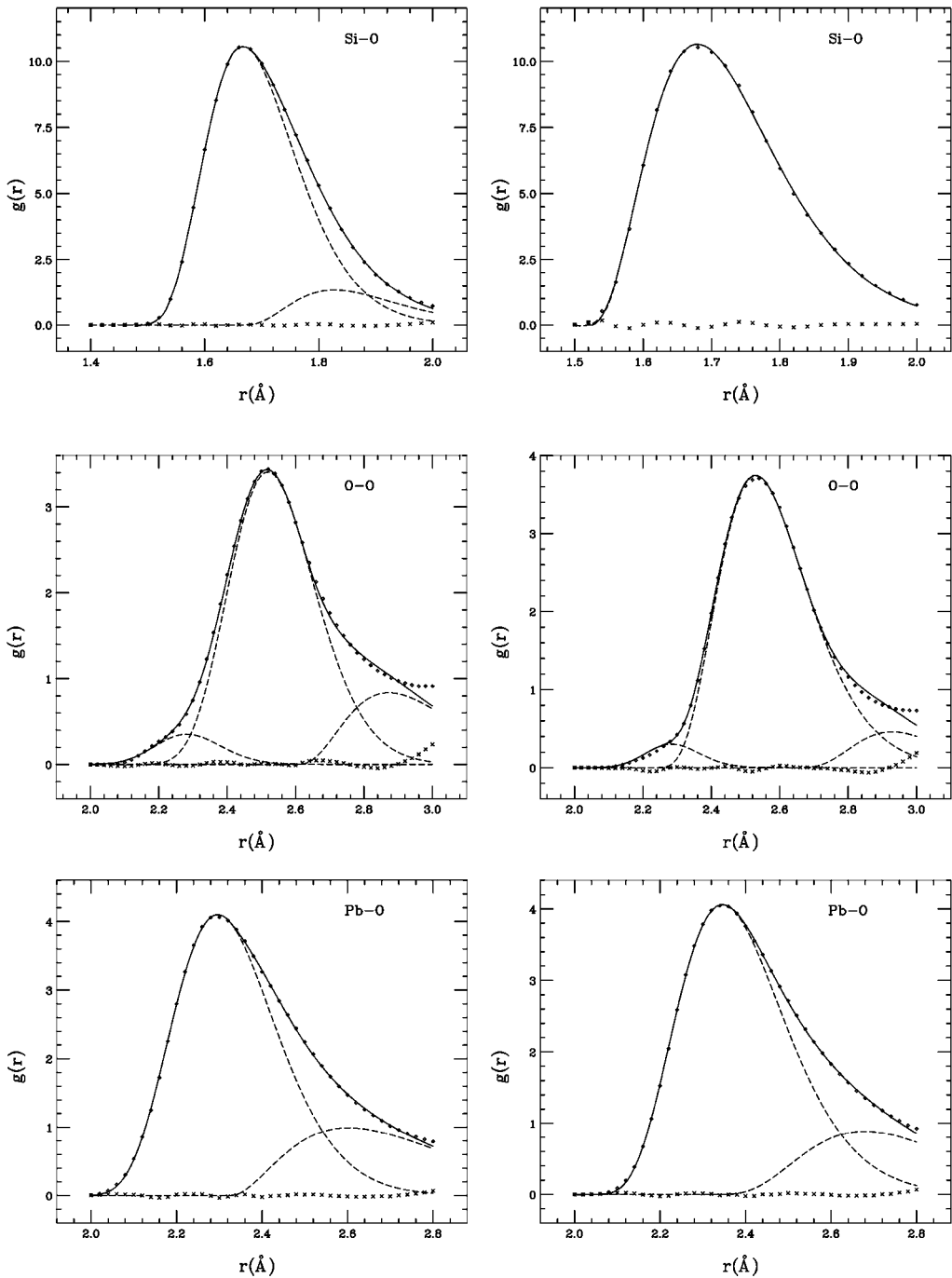


Fig. 9. Si-O, O-O, and Pb-O spatial correlations in dense glasses. The left column corresponds to collapsed PbSiO_3 glass of initial density of 1200 kg/m^3 and final density of $\rho = 8250 \text{ kg/m}^3$. The right column corresponds to $\rho = 8250 \text{ kg/m}^3$ glass quenched from initial hot melt of the same density

Table 5. Structural parameters of the first maxima of pair radial distribution functions in bulk glass ($\rho = 8250 \text{ kg/m}^3$), obtained as a result of spontaneous densification of the $\rho = 1200 \text{ kg/m}^3$ system

Atom pair	$R [\text{\AA}]$	N	$\sigma^2 [\text{\AA}^2]$	β	N_c
Si–O	1.71	4.16	0.008	0.739	4.913
	1.89	0.76	0.013	1	
O–O	2.3	0.3	0.009	0.207	
	2.56	4.7	0.017	0.444	6.999
	2.99	2	0.037	1.001	
Pb–O	2.35	4.57	0.017	0.586	7.072
	2.78	2.5	0.065	1.129	
Si–Si	2.99	1.14	0.023	0.635	
	3.26	2.49	0.014	0.079	4.186
	3.69	0.85	0.058	1.436	
Pb–Pb	3.24	2.95	0.049	0.141	
	3.59	1.31	0.028	0.355	6.645
	4.19	2.38	0.141	1.151	
Pb–Si	3.31	4.52	0.059	0.549	6.582
	3.87	2.06	0.08	0.8	

The average O–O distance amounts to 2.56 Å. This value, considered together with the average Si–O distance of 1.71 Å, explains the appearance of the 90° O–Si–O angle, dominating in the O–Si–O angular distribution (see Fig. 10). The Pb–O distance equal to 2.3 Å, considered together with the O–O distance, suggests the existence of O–O–Pb angles close to 57° (cf. Fig. 10). The Pb–O coordination numbers are distributed in the following way: 6-, 7-, 8-fold coordinations occur in about 30%, 40% and 20%, respectively. There are also some PbO_5 and PbO_9 groups (8% and 5%, respectively). 72% of the basal Pb–O–Pb–O–..'s are 2-member, and 18% - 3-member ones.

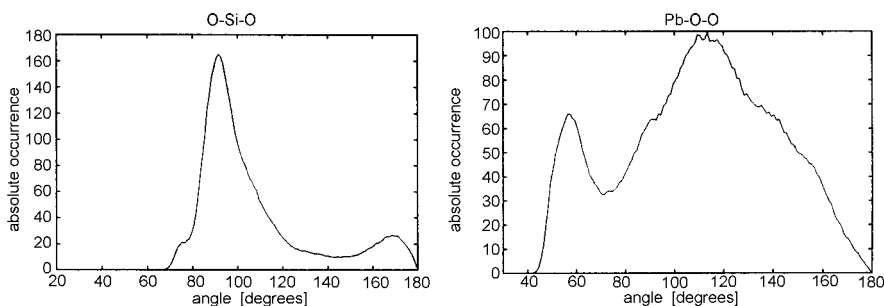


Fig. 10. O–Si–O and Pb–O–O angular distribution functions in a dense system collapsed from initial density of 1200 kg/m^3

Comparing the above described structure of dense (spontaneously collapsed) glasses with the structure of the corresponding initial low-density systems one should note as follows (cf. Tables 5 and 2-4):

1. An increase of the coordination numbers: by almost 3 for Pb-Si and Pb-O pairs and by 1 for Si-O (SiO_4 tetrahedra change to SiO_5 triangular bipyramids).
2. Variations in the average interatomic distances. Due to the increase of the Si-O coordination number, the average Si-O distance increases and the average O-O distance decreases. At the same time average Pb-O bond lengths remain almost density independent.
3. Significant changes in several interbond angular distributions (e.g. the most probable O-Si-O angle decreases from 107° to 97° , the most probable Si-O-Si angle decreases from 171° to 144° , and the most probable Pb-O-Pb angle decreases from 94° to 86°).

Let us finally compare the structure of the spontaneously densified glass with the structure of the glass of the same density obtained by slow cooling from hot dense melt in an (NVT) simulation.

A $PbSiO_3$ system of density $\rho = 8250 \text{ kg/m}^3$ has been well equilibrated at the temperature of 10000 K and then slowly cooled down to room temperature, passing the temperatures of 8000, 6000, 5000, 4000, 3500, 3000, 2500, 2000, 1500, 1000 and 600 K. At each of those temperatures the system was equilibrated during 30000 time steps and sampled during 10000 time steps. Such a scheme corresponds to the cooling rate of about 10^{13} K/s. The structural data for this system are presented in the right-hand columns of Figs. 9 and 11 and in Table 6. The most probable Si-O, O-O and Pb-O distances are 1.68 Å, 2.52 Å and 2.35 Å, respectively. The most probable Si-O-O and O-Si-O angles equal 42° and 96° , respectively.

Table 6. Structural parameters for $\rho = 8250 \text{ kg/m}^3$ $PbSiO_3$ glass obtained by cooling from melt under constant volume conditions

Atom pair	$R [\text{\AA}]$	N	$\sigma^2 [\text{\AA}^2]$	β	N_c
Si-O	1.75	4.921	0.013	0.991	4.921
	2.29	0.2	0.006	0.202	
O-O	2.6	3.58	0.022	0.784	6.958
	2.99	0.88	0.022	0.8	
Pb-O	2.41	4.81	0.019	0.706	6.985
	2.8	2.00	0.045	0.906	
Si-Si	2.95	0.5	0.012	0.015	4.195
	3.31	3.19	0.018	0.446	
Pb-Pb	3.64	0.49	0.039	1.358	6.703
	3.27	2.21	0.026	0.068	
Pb-Si	3.59	1.63	0.022	0.534	6.94
	4.04	1.85	0.073	1.104	
	3.43	5.71	0.06	0.638	
	4	1.23	0.06	0.899	

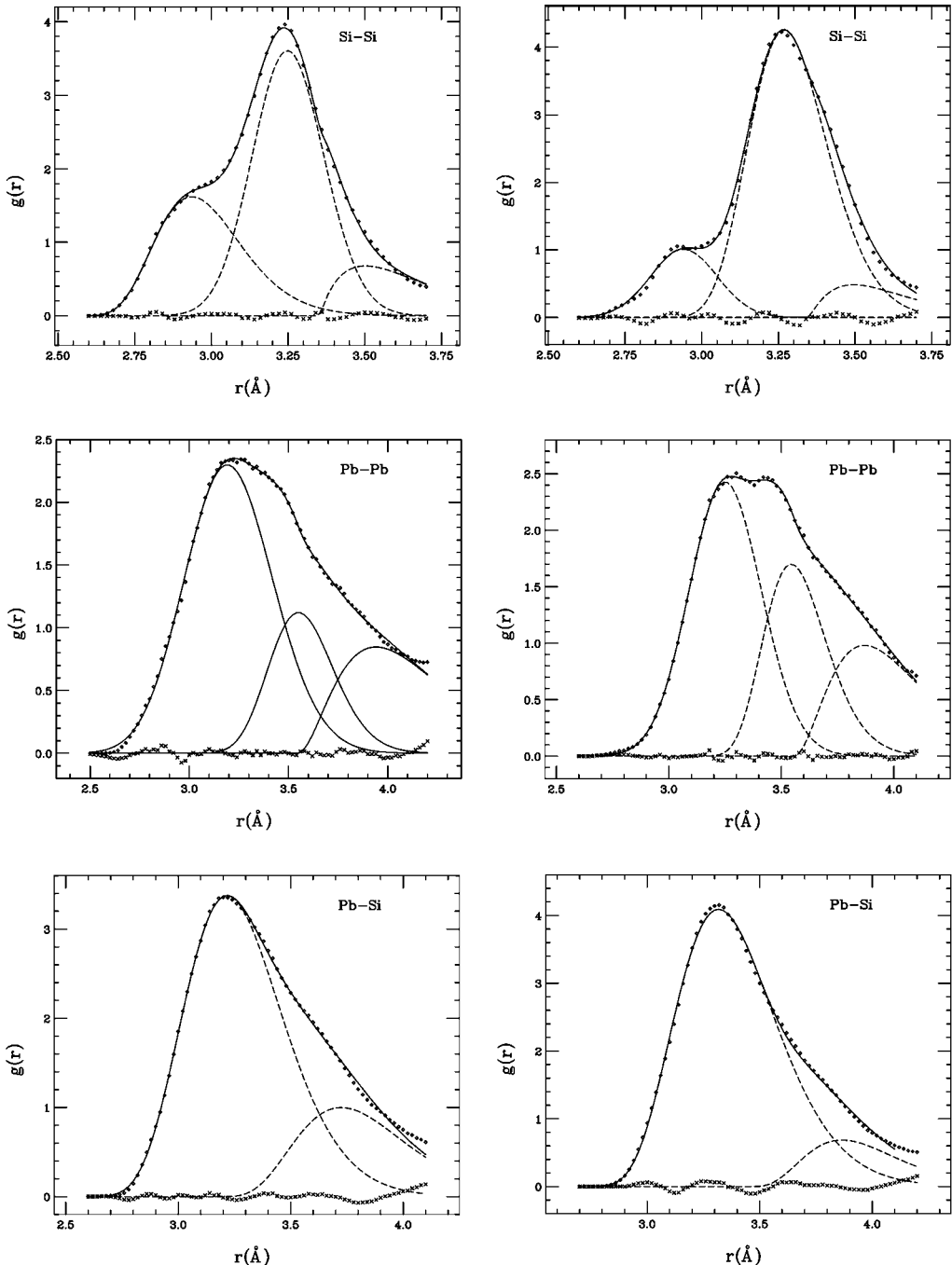


Fig. 11. Si-Si, Pb-Pb and Pb-Si spatial correlations in dense glasses. The left column corresponds to collapsed PbSiO_3 glass of initial density of 1200 kg/m^3 and final density of $\rho = 8250 \text{ kg/m}^3$. The right column corresponds to $\rho = 8250 \text{ kg/m}^3$ glass quenched from initial hot melt of the same density

Comparing the structure of $\rho = 8250 \text{ kg/m}^3$ glass obtained by spontaneous collapse of $\rho = 1200 \text{ kg/m}^3$ glass with that of $\rho = 8250 \text{ kg/m}^3$ glass prepared by slow cooling from the melt of the same density, one should note that:

1. The most probable and average interatomic distances, angular distributions and coordination numbers for the first neighbours are essentially the same for both systems. This suggests that the basic structural units are also the same.
2. The similarity of the cation-anion ring statistics suggests similar medium-range ordering of both systems.
3. The latter conclusion is supported by the fact that the cation-cation (Si-Si, Pb-Pb and Pb-Si) spatial correlations also reveal a high degree of similarity, see Fig. 11.

Thus, both ways of obtaining the high-density phases, i.e. spontaneous densification from a low-density state and slow cooling from hot dense melt, lead to glasses of the same structure.

5. CONCLUDING REMARKS

In this work we have proposed a new "gel-drying" method of obtaining low-density (porous) oxide systems. The method consists in a gradual increase of initially screened ionic charges to their full values under constant volume conditions. The method has been proven to work for PbSiO₃ systems. However, the final low-density structures collapse spontaneously under (NpT) conditions with null external pressure. As a result one obtains high-density homogeneous structures. High-density collapsed PbSiO₃ systems have the same structure as same-density systems prepared from dense melt. Whether this interesting result might be extended to other systems remains to be seen until performing simulations for other compounds.

Moreover, the structures of low-density (porous) and high-density (densified) PbSiO₃ phases have been described and compared in the paper. A detailed comparison of the structure of densified PbSiO₃ glasses with the structure of the same glass at normal density, i.e. 5970 kg/m³, has been presented in [9] and has not been repeated here.

Acknowledgements

The MD simulations were performed at the TASK Supercomputer Centre (Gdansk, Poland). The work has been partially sponsored by KBN, under grants 7 T11F 013 21 and 4 T11F 019 25.

References

- [1] W. G. Hoover, *Molecular Dynamics*, Lecture Notes in Physics, Springer-Verlag, Berlin, Heidelberg, New York **258** (1986).
- [2] M. P. Allen and D. J. Tildesley, *Computer Simulation of Liquids*, Oxford (1997).
- [3] R. W. Hockney and J. W. Eastwood, *Computer Simulations Using Particles*, Moscow (in Russian) (1987)
- [4] C. R. A. Catlow, *Computer Simulation of Solids*, Lecture Notes in Physics, Springer-Verlag, Berlin, Heidelberg, New York, **166** (1982).

- [5] D. C. Rapaport, *The Art of Molecular Dynamics Simulation*, Cambridge (1995).
- [6] A. Rybicka, J. Rybicki, A. Witkowska, S. Feliziani, and G. Mancini, Comput. Meth. Sci. Technol. **5**, 67 (1999).
- [7] J. Rybicki, A. Rybicka, A. Witkowska, G. Bergmański, A. Di Cicco, M. Minicucci, and G. Mancini, J. Phys. CM **13**, 9781 (2001).
- [8] J. Rybicki, A. Witkowska, G. Bergmański, G. Mancini, and S. Feliziani, *The structure of Pb-PbO-SiO₂ glass via molecular dynamics*, TASK Quart. **7**, 243 (2003).
- [9] G. Bergmański, M. Białoskórski, M. Rychcik-Leyk, A. Witkowska, J. Rybicki, G. Mancini, S. Frigio, and S. Feliziani, TASK, Quart. **8**, (3) 393 (2004)..
- [10] A. Rybicka, *The Structure and properties of lead-silicate and lead-germanate glasses*, PhD Thesis, Politechnika Gdańsk (1999).
- [11] <http://www.uci.agh.edu.pl/alda/mdsim>.
- [12] A. Filipponi and A. Di Cicco, Phys. Rev. B **51**, 12322 (1995).
- [13] A. Filipponi, J. Phys. Cond. Matter **13**, R23 (2001).
- [14] D. S. Yang, D. R. Fazzini, T. I. Morrison, L. Troger, and G. Bunker, J. Non-Cryst. Solids **210**, 275 (1997).
- [15] G. Bergmański, J. Rybicki, and G. Mancini, TASK Quart. **4**, 555 (2000).
- [16] J. Rybicki, G. Bergmański, and Mancini, J. Non-Cryst. Solids **293-295**, 758 (2001).
- [17] <http://www.task.gda.pl/software/anelli>,
- [18] G. Mancini, TASK Quart. **1**, 89 (1997).
- [19] R. Balducci and R. S. Pearlman, J. Chem. Inf. Comput. Sci. **34**, 822 (1994).
- [20] G. Mancini, J. Phys. Commun. **143**, 187 (2002).